REJUVENATION RESEARCH
Volume 21, Number 4, 2018
Mary Ann Liebert, Inc.
DOI: 10.1089/rej.2017.1971

Prunella vulgaris L. Exerts a Protective Effect Against Extrinsic Aging Through NF-κB, MAPKs, AP-1, and TGF-β/Smad Signaling Pathways in UVB-Aged Normal Human Dermal Fibroblasts

Mengyang Zhang, Eunson Hwang, Pei Lin, Wei Gao, Hien T.T. Ngo, and Tae-Hoo Yi

Abstract

Prunella vulgaris L., a well-known traditional Chinese herbal medicine, has anti-inflammatory and antioxidant activities. In the present study, the underlying molecular mechanisms of the protective effect of *P. vulgaris* extract (PVE) were investigated in UVB-irradiated normal human dermal fibroblasts (NHDFs). The mRNA expression of matrix metalloproteinases (MMPs), procollagen type I, and cytokines, such as interleukin-6 (IL-6) and tumor necrosis factor (TNF-α), was determined by reverse transcription–polymerase chain reaction. The expression of anti-photoaging-related signaling molecules in the NF-κB, MAPK/AP-1, and TGF/Smad pathways was assessed by western blot. We observed that PVE blocked the upregulated production of radical oxygen species induced in UVB-irradiated NHDFs in a dose-dependent manner. Treatment with PVE also significantly ameliorated the mRNA levels of MMPs, procollagen type I, TNF-α, and IL-6. In addition, the phosphorylation level of c-Jun and c-Fos was decreased through the attenuated expression levels of p-ERK and p-JNK after treatment with PVE. Furthermore, cells treated with PVE showed inhibited Smad 7 and increased Smad 2/3 expression in the TGF-β/Smad signaling pathway. Hence, synthesis of procollagen type I, a precursor of collagen I, was promoted. These findings indicate that treatment with PVE has a potential protective effect against UVB-induced photoaging and photoinflammation.

Keywords: *P. vulgaris* L., NF-κB, MAPK, AP-1, TGF-β/Smad, collagen I

Introduction

Skin changes are the most obvious characteristic of aging, and are associated with environmental factors and genetic makeup, as well as lifestyle and dietary habits. The greatest environmental factor is chronic exposure to solar ultraviolet (UV) light. Extensive epidemiological evidence indicates that UVB irradiation (290–320 nm) is the major factor that causes skin damage, such as sunburn, inflammation, photoaging, and even cancer.[1]

Chronic exposure to UVB leads to abnormal production of radical oxygen species (ROS), which stimulate multiple cell surface cytokines, growth factor receptors, and mitogen-activated protein kinases (MAPKs). MAPKs participate in regulating cellular responses to different stimuli and have various cell functions, including proliferation, differentiation, cell survival, and apoptosis.[2–4] Previous research has demonstrated that activation of MAPKs occurs through the phosphorylation of extracellular-regulated protein kinase (ERK), Jun N-terminal kinase (JNK), and p38 signaling pathways.[5,6] Since the activated MAPKs are translocated to the nucleus, activator protein 1 (AP-1) is also phosphorylated as a downstream MAPK transcription factor,[5] followed by upregulation of the expression of matrix metalloproteinases (MMPs).[7] MMPs are a family of zinc-dependent endopeptidases involved in the breakdown of the extracellular matrix (ECM) in physiological processes. In aged skin, the reduced size of fibroblasts is accompanied by their decreased production of key ECM components, such as type I collagen, fibronectin, and connective tissue growth factor.[8]

College of Life Sciences, Kyung Hee University, Yongin-si, Republic of Korea.

Transforming growth factor-β1 (TGF-β1), a multifunctional cytokine, plays a fundamental role in regulating cellular processes and the production of various ECM components, including collagen, elastin, and fibronectin. Many of the dermal ECM-related genes that are downregulated in aged human skin are regulated by the TGF-β pathway.[9] Recent studies have identified Smad proteins as major downstream targets of activated TGF-β receptor kinases. Importantly, components of the TGF-β pathway itself are reduced in aged human skin,[10] raising the possibility that impairment of TGF-β signaling may be a major contributor to reduced ECM production in aged skin.

Cutaneous homeostasis is maintained by permanent crosstalk between dermal fibroblasts and epidermal keratinocytes, and through the production of cytokines.[11] UVB irradiation induces activation of transcription factor nuclear factor kappa B (NF-κB) in the skin cells, thus inducing the expression of MMPs and cytokines.[12] NF-κB is an important transcription factor that is activated by the transcription of proinflammatory mediators, such as interleukin-6 (IL-6) and tumor necrosis factor (TNF-α), which are involved in the activation of inflammatory and oxidative stress.[13]

Pharmacotherapy plays an important role in addressing aging skin. Our previous studies indicate that natural products can downregulate UVB-induced MMP-1 expression by inhibiting activation of the MAPK and AP-1 pathways,[14–16] thereby offering an effective method to relieve photoaging. *Prunella vulgaris* L. is a widely distributed perennial herb, and the dried spica of *P. vulgaris* is traditionally used as an herbal medicine to alleviate fever, reduce sore throats, and accelerate wound healing. Modern *in vitro* and *in vivo* clinical studies suggested that *P. vulgaris* has a wide spectrum of biological effects, including antiviral, antitumor, and anti-inflammatory stimulation of the immune system and enhancement of production of T-lymphocytes and cytokines.[17]

P. vulgaris is a well-known Chinese traditional medicine with many useful pharmacological activities. However, its applicability for treating UVB-induced photoaging and photoinflammation has not been studied. Accordingly, we investigated the effect of *P. vulgaris* extract (PVE) on UVB-induced damages in the present study.

Materials and Methods

Preparation and characterization of PVE

Dried flower spikes of *P. vulgaris* were purchased from Mountain Rose Herbs (Eugene, OR). The dried spikes were crushed into a thin powder and extracted three times for 24 hours at 37°C in 50% ethanol with a ratio of 1:50 (w/v), then filtered and concentrated using a rotating vacuum evaporator at 40°C. The extract of *P. vulgaris* was lyophilized and stored at −20°C. The lyophilized powder was dissolved in 10% dimethyl sulfoxide and filtered through a 0.22-μm syringe filter to make the stock solution.

To ascertain the quality and ensure the purity of the PVE, high-performance liquid chromatography (HPLC) was performed on a Dionex Chromelon™ chromatography data system with P580 and UVD100 detectors (Thermo Fisher Scientific, Inc., Waltham, MA). Chromatographic separation was performed on a Waters SunFire C18 column (250×4.6 mm, 5-μm particle size). Elution was performed with a methanol/acetonitrile (3:1) gradient containing 1% formic acid. The gradient was increased linearly from 10% to 90% methanol over 35 minutes. The injection volume was 10 μL and the flow rate was 1 mL/min.

Chemicals

ELISA Kits for MMP-1, MMP-3, and IL-6 were purchased from R&D Systems, Inc. (Minneapolis, MN). Dulbecco's modified Eagle's medium (DMEM), fetal bovine serum (FBS), and penicillin–streptomycin were purchased from Gibco BRL (Grand Island, NY). Unless otherwise mentioned, solvents were purchased from Samchun Chemicals (Seoul, Korea), and inorganic salts from Sigma-Aldrich (St. Louis, MO).

Cell culture and UVB irradiation

NHDFs, normal human dermal fibroblasts (MCTT Core, Inc., Seoul, Korea), were cultured in DMEM supplemented with 10% heat-inactivated FBS and 1% penicillin–streptomycin. Cells were grown at 37°C in a humidified atmosphere containing 5% CO_2. Monolayer cultures of NHDFs were subjected to irradiation at a dose of 144 mJ/cm^2 using a UVB source (Bio-Link BLX-312; Vilber Lourmat, Gmbh, France) set to a spectral peak at 312 nm.[14] All experiments were performed using cells with no more than 10 passages.

MTT assay

Cell viability was determined by MTT assay. Briefly, logarithmic-phase NHDFs were counted and seeded in 96-well culture plates. After 72 hours of treatment with PVE (1, 10, 100 μg/mL), the medium was removed and MTT (100 μg/mL) was added, followed by 4 hours of incubation. Cells were then washed in triplicate with PBS and DMSO added to dissolve the formazan crystals. The absorbance was read at 570 nm using a microplate reader (Molecular Devices E09090; San Francisco, CA). Each sample was determined six times.

Measurement of 2,2-diphenyl-1-picrylhydrazyl radicals and ROS scavenging ability

2,2-Diphenyl-1-picrylhydrazyl (DPPH) was introduced to measure the antioxidant ability of the PVE. Arbutin was used as a positive control. Following UVB (144 mJ/cm^2) irradiation and treatment with PVE for 24 hours, NHDFs were stained with 30 μM 2′7′-dichlorofluorescein diacetate (DCFH-DA; Sigma-Aldrich) for 30 minutes at 37°C. Cells were then washed twice with PBS and analyzed using a multimode microplate reader (Molecular Devices Filter Max F5, Sunnyvale, CA).

Reverse transcription–polymerase chain reaction

RNA was isolated from NHDFs treated with PVE (1, 10, 100 μg/mL) for 24 hours following UVB irradiation according to the manufacturer's instructions using TRIzol reagent (Invitrogen Life Technologies, Carlsbad, CA). Polymerase chain reaction (PCR) amplification of the cDNA template was performed using PCR premix (Bioneer) and the following primer pairs: MMP-1, forward 5′-TGC GCA CAA ATC CCT TCT-3′, reverse 5′-TTC AAG CCC ATT TGG CAG TT-3′; MMP-3, forward 5′-GGCCAGGGATTAATGGAGAT-3′, reverse 5′-GGAACCGAGTCAGGTCTGTG-3′. Procollagen type I,

forward 5′-CTC GAG GTG GAC ACC CT-3′, reverse 5′-CAG CTG GAT GGC CAC ATC GG-3′; TNF-α, forward 5′-AGGG GAAATGAGAGACGCAA-3′, reverse 5′-TTCCCCATCTCT TGCCACAT-3′; IL-6, forward 5′-CTCCTTCTCCACAAGCG CC-3′, reverse 5′-GCCGAAGAGCCCTCAGGC-3′; and glyc eraldehyde-3-phosphate dehydrogenase (GAPDH), forward 5′-ACC ACA GTC CAT GCC ATC AC-3′, reverse 5′-CCA CCA CCC TGT TGC TGT AG-3′. Reverse transcription–PCR (RT-PCR) was performed in a Veriti Thermal Cycler (Applied Biosystems, Foster City, CA) as previously described.[14] PCR products were stained with nucleic acid staining solution and separated by 2.0% agarose gel. Each experiment was repeated at least three times.

Measurement of MMPs and IL-6 production

Logarithmic-phase NHDFs were counted and seeded in six-well culture plates, and after 72 hours of treatment with PVE (1, 10, 100 μg/mL), the cell medium was collected from each well. MMP-1, MMP-3, and IL-6 levels were measured in the media using commercially available ELISA Kits in accordance with the manufacturer's instructions. Each sample was measured in triplicate.

Western blot analysis

NHDFs were treated with UVB irradiation (144 mJ/cm^2) and PVE (1, 10, 100 μg/mL) and then checked for alterations in the level of signaling molecules in the MAPK/AP-1, NF-κB, and TGF/Smad pathways, respectively. Cells were lysed using RIPA Lysis buffer (Cell Signaling Technology, Danvers) and the protein concentration was measured using Bradford reagent (Bio-Rad, Hercules, CA) as described by the manufacturer. The proteins were separated on 10% SDS-PAGE and transferred onto PVDF membranes. The membrane was incubated with various primary antibodies after blocking. Protein bands were visualized with enhanced chemiluminescence detection reagents after hybridization with HRP-conjugated secondary antibodies. Antibodies against ERK, phosphor-ERK, JNK, phosphor-JNK, p38, and phosphor-p38, as well as anti-rabbit-HRP and anti-mouse-HRP antibodies were purchased from Cell Signaling Technology, and those against NF-κB p65, c-Fos, phosphor-c-Fos, c-Jun, phosphor-c-Jun, TGF-β1, Smad2/3, phosphor-Smad2/3, Smad7, and β-actin were purchased from Santa Cruz Biotechnology (Dallas). Each experiment was repeated at least three times.

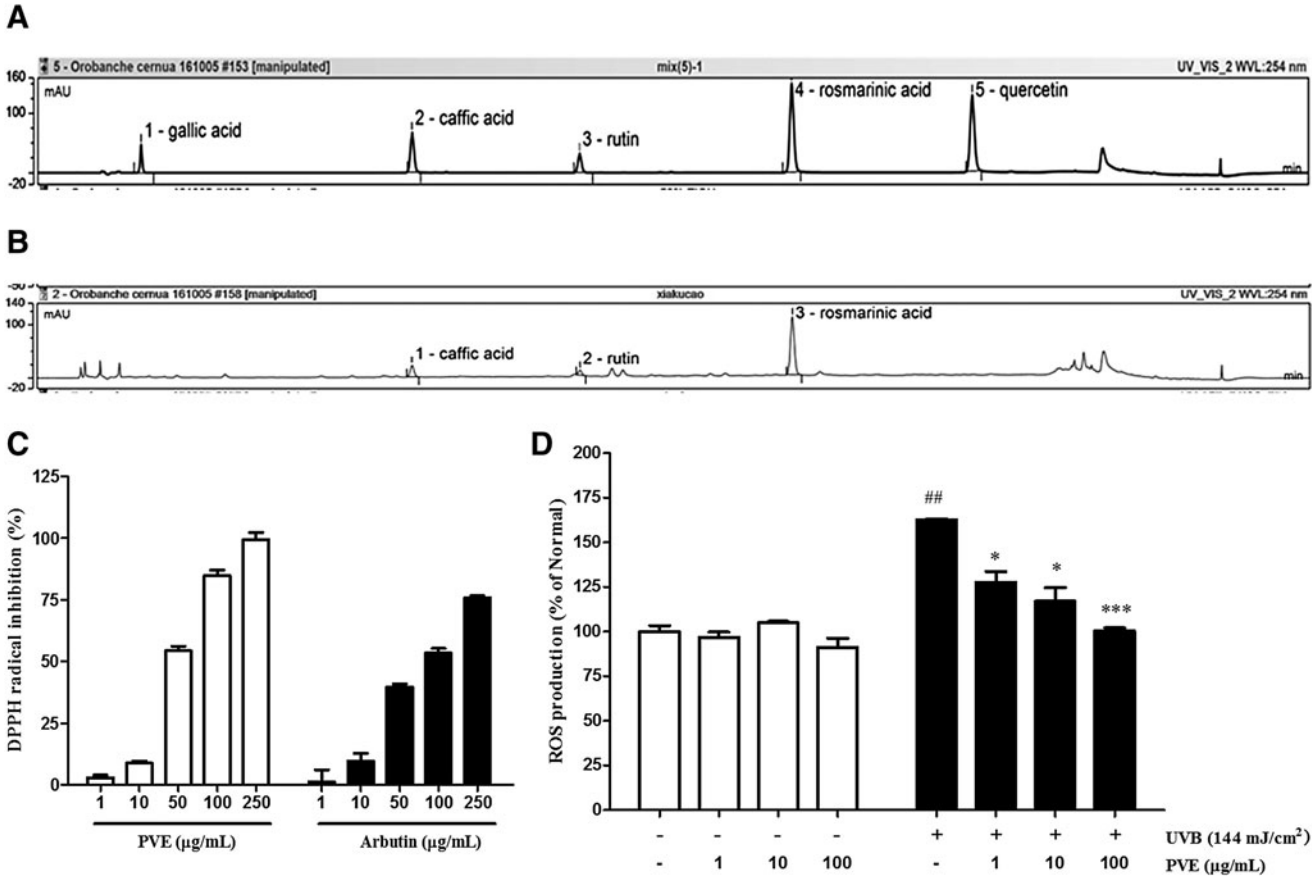

FIG. 1. HPLC analysis and antioxidant activity of PVE. **(A)** Standard of gallic acid, caffeic acid, rutin, rosmarinic acid, and quercetin. **(B)** PVE. **(C)** DPPH scavenging activity. Arbutin was used as a positive control. Values are mean ± SD. **(D)** Intracellular ROS scavenging activity. ROS generation levels were determined after 24 hours of UVB irradiation and treatment of PVE. Values are mean ± SD. Relative ROS generation of cells is shown in each histogram. * indicates significant differences between nonirradiated control and UVB-irradiated control, respectively. $^{\#\#}p < 0.01$, versus nonirradiated control. $^{*}p < 0.05$, $^{***}p < 0.001$, versus UVB-irradiated control. DPPH, 2,2-diphenyl-1-picrylhydrazyl; HPLC, high-performance liquid chromatography; PVE, *P. vulgaris* extract; ROS, radical oxygen species; SD, standard deviation.

Statistical analyses

Data are presented as mean ± standard deviation of three independent experiments in triplicate. Student's *t*-tests were performed to compare individual treatments to controls, and comparisons between different treatments were analyzed employing one-way analysis of variance with a significance level of $p < 0.05$.

Results

Analysis of PVE

To prepare PVE, the dried spica of *P. vulgaris* (15 g) was extracted in 50% ethanol resulting in a crude product yield of 11.9% (1.19 g). As shown in Figure 1A and B, the main compounds of rosmarinic acid 1.49%, caffeic acid 0.33%, and rutin 0.11% were identified.

Antioxidant activity of PVE

The free radical-scavenging activity of PVE and arbutin was determined by DPPH assay. As shown in Figure 1C, their free radical inhibition activity increased in a dose-dependent manner. In addition, the antioxidant activity of PVE to scavenged DPPH radicals was superior to that of arbutin, the positive control. In particular, the IC_{50} values of arbutin and PVE were 93.64 and of 46.0 μg/mL, respectively.

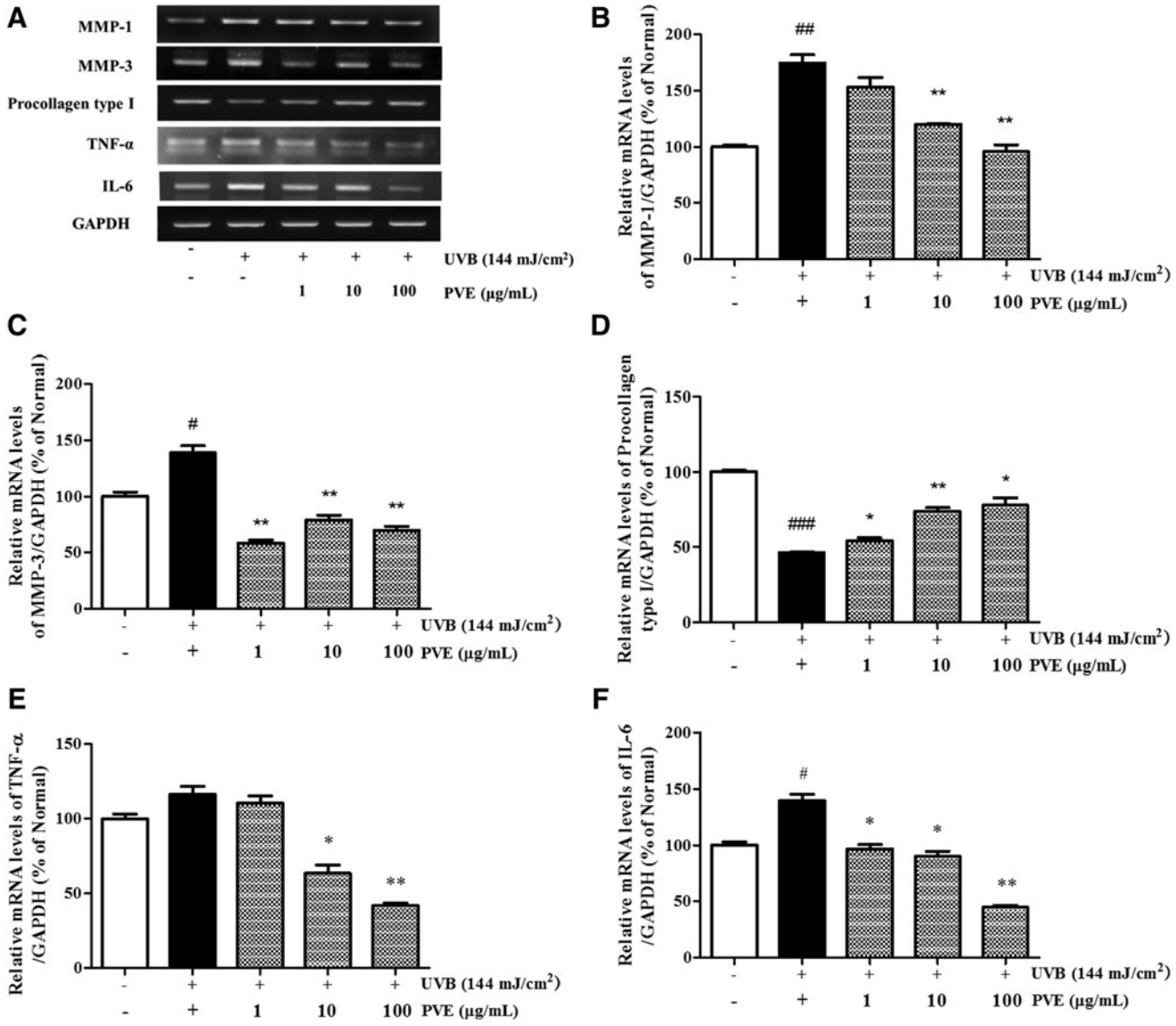

FIG. 2. mRNA expression level **(A)** of MMPs **(B, C)**, procollagen type I **(D)**, TNF-α **(E)**, and IL-6 **(F)** in UVB-irradiated and PVE-treated NHDFs. NHDFs were irradiated with UVB (144 mJ/cm^2) followed by treatment with PVE (1, 10 and 100 μg/mL) for 24 hours. GAPDH mRNA was used as an internal control. Band intensities were quantified by densitometry, normalized to the level of GAPDH mRNA, and calculated as the percentage of the basal response. Values are mean ± SD. $^{\#}p < 0.05$, $^{\#\#}p < 0.01$, $^{\#\#\#}p < 0.001$, versus nonirradiated control. $^{*}p < 0.05$, $^{**}p < 0.01$, versus UVB-irradiated control. GAPDH, glyceraldehyde-3-phosphate dehydrogenase; IL-6, interleukin-6; MMPs, matrix metalloproteinases; NHDFs, normal human dermal fibroblasts.

UVB-induced ROS production in NHDFs was investigated by FACS analysis. As expected, UVB-irradiated cells notably enhanced ROS generation when compared with nonirradiated cells. The increased ROS level was quenched by 38% treatment with PVE at 100 μg/mL compared with cells treated with radiation only (Fig. 1D).

Role of PVE in mRNA expression of MMPs, procollagen type I, TNF-α, and IL-6 in UVB-induced NHDFs

UVB-activated MMP secretion is a hallmark of aging skin. As shown in Figure 2, mRNA levels of MMPs were increased by UVB irradiation. In cells treated with PVE, MMP-1 mRNA expression decreased in a dose-dependent fashion, whereas expression levels of MMP-3 mRNA did not. The mRNA level of MMP-3 was lower at 1 μg/mL PVE than that at 10–100 μg/mL PVE. Procollagen type I is the primary constituent of the ECM, and its reduction is closely associated with aging skin. The mRNA level of procollagen type I in UVB-irradiated NHDFs was significantly diminished compared with nonirradiated cells. With PVE treatment, the expression level of UVB-reduced procollagen type I was improved in a dose-dependent manner.

To investigate whether PVE could inhibit the inflammatory response induced by UVB irradiation, RT-PCR was performed to detect the mRNA levels of TNF-α and IL-6. As shown in Figure 2, PVE effectively reduced the levels of TNF-α and IL-6 mRNA in NHDFs treated with PVE at 100 μg/mL compared with cells treated with radiation only.

Inhibition of MMP and IL-6 production in UVB-irradiated and PVE-treated NHDFs

To determine the effect of PVE on cellular viability, NHDF cells were treated with different concentrations of PVE (1, 10, 100 μg/mL) and analyzed using the MTT assay. Cells treated with PVE showed no significant change in cell viability compared with nonirradiated cells (Fig. 3A).

As shown in Figure 3B and C, UVB irradiation led to an abnormal elevation in MMP-1 and MMP-3 production that was remarkably altered after treatment with PVE. These data agreed with the ELISA results. In particular, PVE at 100 μg/mL inhibited the expression of MMP-1 and MMP-3 by 67.6% and 75.0%, respectively. In the same process, UVB irradiation also induced the production of proinflammatory cytokine IL-6. Treatment with PVE significantly attenuated the secretion of IL-6, with inhibition occurring in a dose-dependent manner (Fig. 3D).

Inhibitory effects of PVE on the UVB-induced phosphorylation of MAPKs

To investigate the effects of PVE on UVB-induced photoaging and photoinflammation, the phosphorylation of MAPKs was assessed. As shown in Figure 4A–D, cells treated with UVB radiation showed only increased phosphorylation of JNK, p38, and ERK compared with nonirradiated cells.

Treatment with PVE at 100 μg/mL provided the most inhibition on phosphorylated MAPKs. In particular, treatment with PVE reduced p-JNK and p-ERK expression by

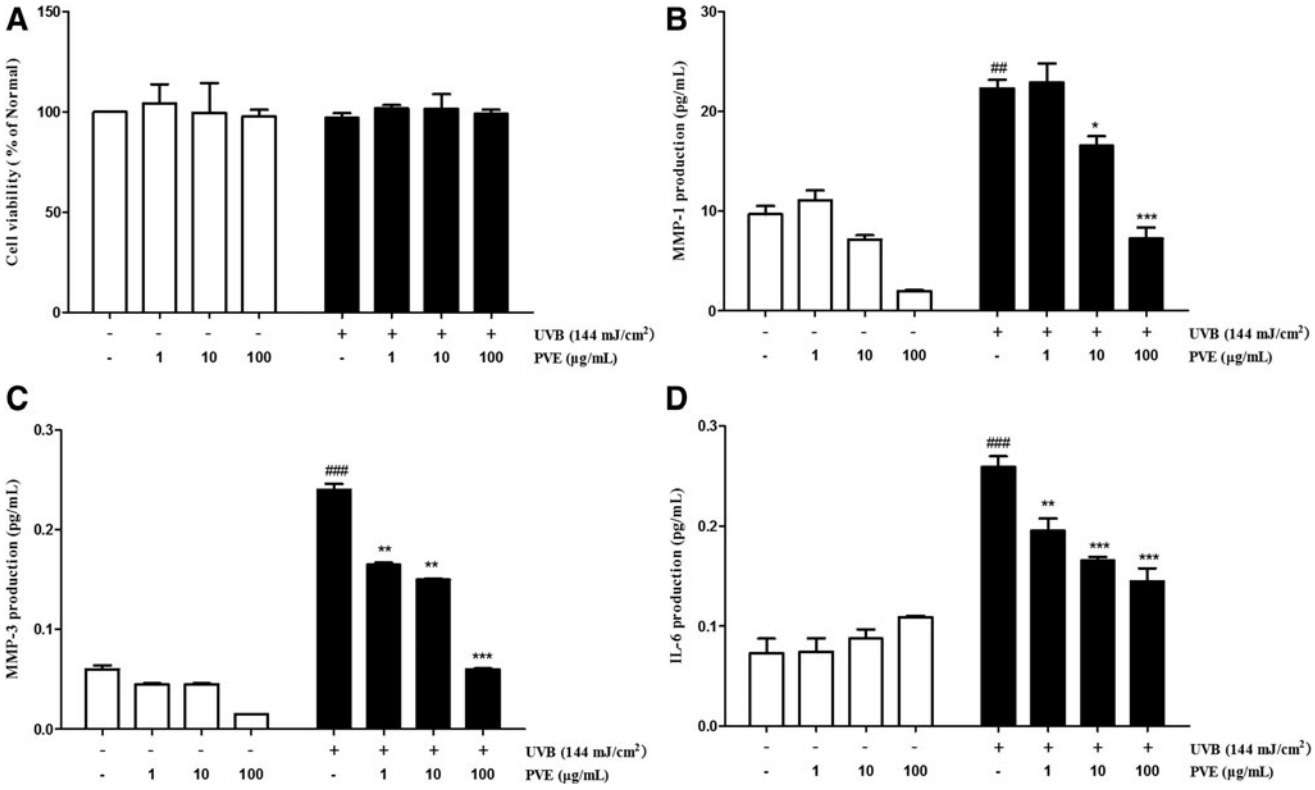

FIG. 3. Cell viability **(A)**, MMPs secretion **(B, C)**, and IL-6 production **(D)** in UVB-irradiated and PVE-treated NHDFs. Treatment with PVE (1, 10, 100 μg/mL) was carried out for 72 hours. Values are mean ± SD. $^{\#\#}p < 0.01$, $^{\#\#\#}p < 0.001$, versus nonirradiated control. $^{*}p < 0.05$, $^{**}p < 0.01$, $^{***}p < 0.001$, versus UVB-irradiated control.

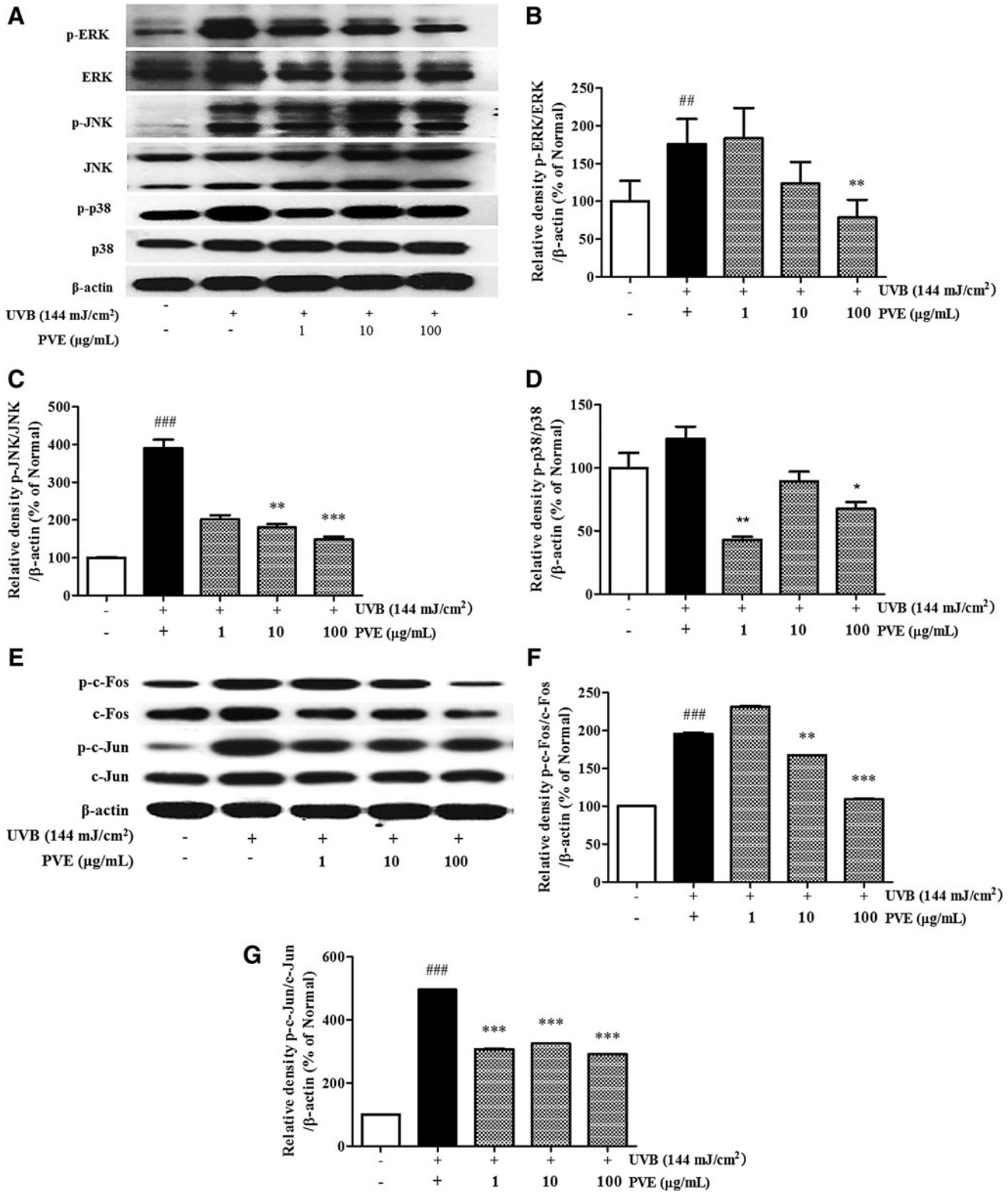

FIG. 4. Inhibitory effect of PVE on MAPKs **(A–D)** and AP-1 **(E–G)**. NHDFs were irradiated with UVB (144 mJ/cm^2) followed by treatment with PVE (1, 10, 100 μg/mL) for 1.5 hours. Phosphorylation and nonphosphorylation of JNK, ERK, p38, c-Fos, and c-Jun were measured. The band intensities were quantified by densitometry, normalized to the level of β-actin, and calculated as the percentage of the basal response. Values are mean ± SD. $^{\#\#}p < 0.01$, $^{\#\#\#}p < 0.001$, versus nonirradiated control. $^{*}p < 0.05$, $^{**}p < 0.01$, $^{***}p < 0.001$, versus UVB-irradiated control. ERK, extracellular signal-regulated kinase; JNK, c-Jun N-terminal kinase; MAPKs, mitogen-activated protein kinases.

62.1% and 55.4%, respectively, in a dose-dependent manner, as well as p-p38 expression at 1 μg/mL.

Inhibitory effects of PVE on UVB-induced phosphorylation of AP-1

The transcription factor AP-1, which is composed of the c-Jun and c-Fos proteins, can be activated by UVB radiation. On the other hand, MMPs are regulated by the AP-1 transcription factor. As shown above, MMPs in PVE-treated cells were decreased compared with cells treated with radiation only. We further investigated the effect of PVE on UVB-induced phosphorylated AP-1. As shown in Figure 4E–G, cells treated with UVB radiation showed only increased phosphorylation of c-Jun and c-Fos compared with nonirradiated cells.

Treatment with PVE inhibited the phosphorylation of c-Jun and c-Fos in a dose-dependent manner. PVE at 100 μg/mL inhibited p-c-Jun and p-c-Fos by 41.1% and 44.3%, respectively, compared with cells treated with radiation only. Accordingly, PVE could inhibit UVB-phosphorylated AP-1 overexpression.

Alleviatory effect of PVE on UVB-induced NF-κB p65 expression

Expression of NF-κB p65, the UVB-induced inflammatory marker, was detected by western blot. Our data showed that PVE significantly alleviated NF-κB p65 protein expression in a concentration-dependent manner compared with cells treated with radiation alone (Fig. 5A, B).

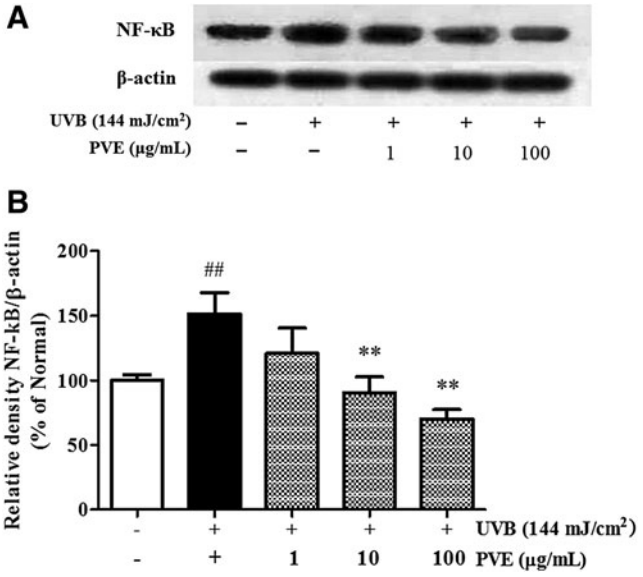

FIG. 5. Inhibitory effect of PVE on the NF-κB p65 signaling pathway **(A, B)**. NHDFs were irradiated with UVB (144 mJ/cm^2) followed by treatment with PVE (1, 10, 100 μg/mL) for 1.5 hours. The band intensities were quantified by densitometry, normalized to the level of β-actin, and calculated as the percentage of the basal response. Values are mean ± SD. $^{\#\#}p < 0.01$, versus nonirradiated control. $^{**}p < 0.01$, versus UVB-irradiated control. NF-κB, nuclear transcription factor kappa B.

Enhancing effect of PVE on the UVB-reduced TGF/Smad signaling pathway

Smad proteins and TGF-β play a pivotal role in TGF-β-dependent regulation of collagen and production of other ECM components. As expected, the levels of TGF-β1 and phosphorylated Smad2/3 were significantly upregulated in cells treated with PVE (Fig. 6). PVE effectively stimulated TGF-β1 expression, promoting the synthesis of procollagen type I (Fig. 2). PVE could retard collagen degradation through regulation of the TGF-β1/Smad 2/3 pathway in UVB-irradiated NHDFs.

Discussion

Skin aging is a natural chronic process of senescence. UVB exposure speeds up chronological skin changes, such as the formation of wrinkles and both structural and functional cell damages. In this process, oxidative stress initiated by ROS generation is an important factor modulating skin alterations and aging.[18] Thus, a natural product with antioxidant, anti-photoaging, and anti-photoinflammation activities is needed to develop.

P. vulgaris L., commonly known as ''self-heal,'' is a widely distributed perennial herb that has been used as a traditional medicine for inflammatory diseases and wound healing.[17] Ethanol extracts of *P. vulgaris* have been reported to have diverse health benefits, including prevention of oxidative stress and the treatment of thrombosis, lipid peroxidation, obesity, hypercholesterolemia, and hyperlipidemia.[19] *P. vulgaris* L. contains a variety of structurally diverse natural products,[20] primarily flavonoids, triterpenoids, and phenolic acids, such as rosmarinic acid (RA), caffeic acid (CA), ursolic acid (UA), oleanolic acid (OA), and rutin (RT), which possess a wide array of biological activities.[21]

In our study, HPLC analysis indicated that 50% ethanol PVE contained 1.49% RA, 0.33% CA, and 0.11% RT, which have been reported to have antioxidative and anti-inflammatory activities. Zdarilová et al.[22] investigated whether RA could reduce ROS production and inhibit LPS-induced IL-1β, IL-6, and TNF-α upregulation, effectively modulating inflammation. CA, as the main component of various plants, relieves proinflammatory responses through the NF-κB pathway[23] and effectively protects human skin from photo-oxidative damage.[24] In our study, PVE showed higher free radical-scavenging activity than arbutin, and inhibited ROS production in a dose-dependent manner. This natural product represents a promising lead compound or an intervention in photo-oxidative and photoinflammation therapy.

During UVB radiation, the system faces disturbance, and several cytokines and growth factors stimulate the transcription of MMPs. Increased MMP-1 protein expression would cause the degradation of types I, II, and III collagen. Inhibition of the expression of procollagen type I, the primary component of the ECM, would destroy the structural integrity of the dermis.[7] Thus, the development of MMP inhibitors or procollagen type I activators is a research hotspot in combating photoaging. In this study, PVE effectively inhibited the secretion of MMPs in UVB-induced NHDFs. Treatment with PVE inhibited UVB-induced MMP-1 mRNA expression in a dose-dependent manner, and significantly reduced the expression of MMP-3 mRNA ($p < 0.01$). PVE had protective

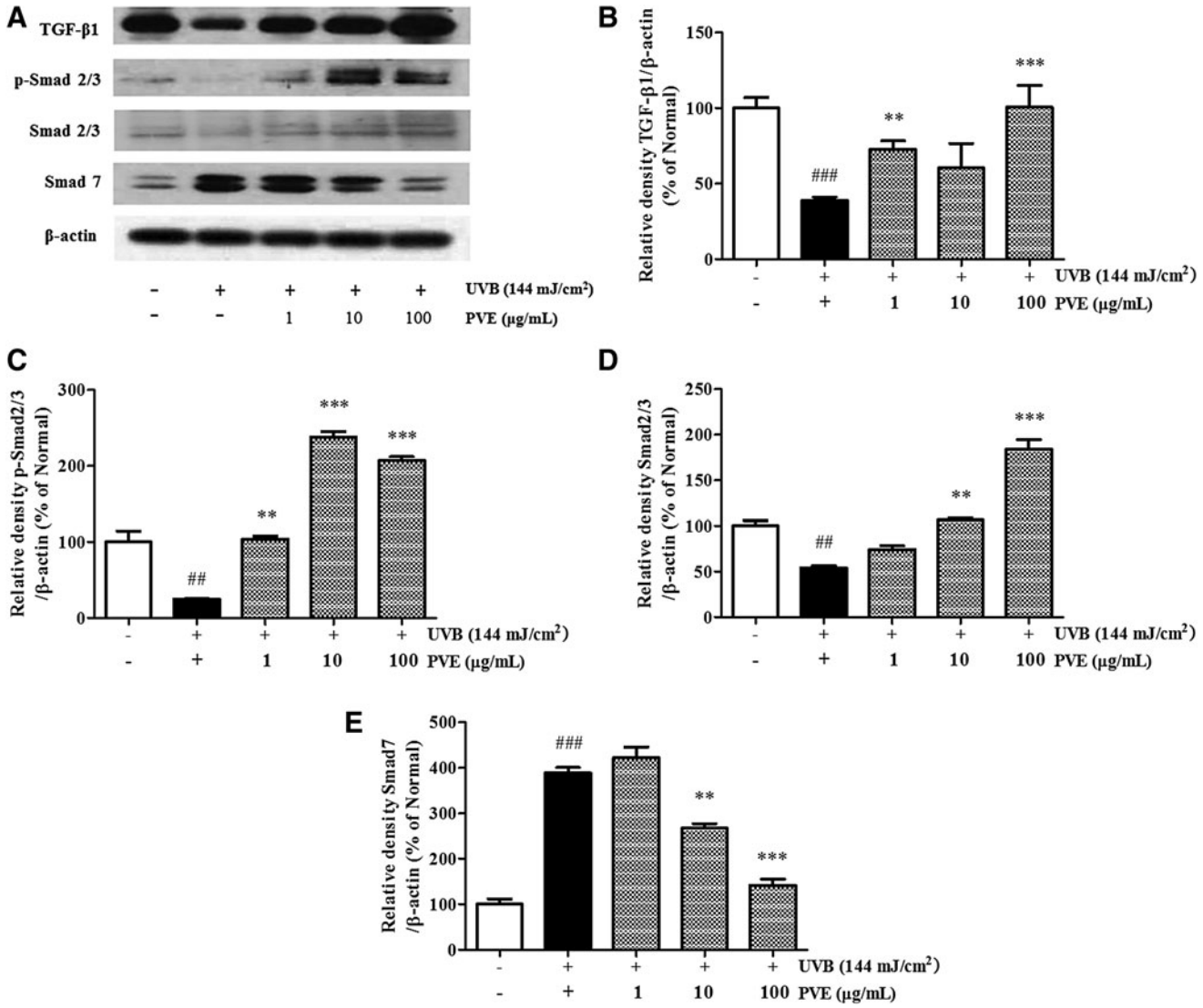

FIG. 6. Enhancing effect of PVE on the TGF/Smad signaling pathway (**A**). NHDFs were irradiated with UVB (144 mJ/cm^2) followed by treatment with PVE (1, 10, 100 μg/mL) for 1.5 hours. The band intensities were quantified by densitometry, normalized to the level of β-actin, and calculated as the percentage of the basal response for TGF-b1 (**B**), p-Smad2/3 (**C**), Smad 2/3 (**D**), and Smad7 (**E**). Values are mean ± SD. $^{\#\#}p < 0.01$, $^{\#\#\#}p < 0.001$, versus nonirradiated control. $^{**}p < 0.01$, $^{***}p < 0.001$, versus UVB-irradiated controls. TGF, transforming growth factor.

effect on reducing MMP expression, and the more prominent role was to improve the level of procollagen type I.

In the human dermis, fibroblasts are embedded in a collagen-rich microenvironment and interact with collagen fibrils to maintain normal cell size and mechanical force.[8] The dermal ECM becomes progressively fragmented during aging. Many of the dermal ECM-related genes that are downregulated in aged human skin are regulated by the TGF-β pathway.[10] Importantly, components of the TGF-β pathway itself are reduced in aged human skin. Recent studies have identified Smad proteins as major downstream targets of activated TGF-β receptor kinases, exerting distinct and opposing functions.[25] As a negative feedback inhibitor, Smad 7 can compete with Smad 2 and Smad 3 for binding to activated TGFR1 and thus reduce TGF-β/Smad signaling.[25,26] In this study, PVE both inhibited the expression of Smad 7 in a concentration-dependent manner, blocking the negative regulation of TGF-β, and significantly stimulated Smad 2/3 phosphorylation, thus renovating TGF-β1 expression to the normal level. We reasonably concluded that PVE restored procollagen type I expression by activating TGF-β1 through the effects of Smad 2/3 promotion and Smad 7 inhibition in NHDFs.

When ROS trigger the activation of MAPK signaling pathways, the JNK and ERK proteins translocate to the nucleus where they phosphorylate c-Jun and c-Fos enhancing their transcriptional activity.[14–16] The contribution of p38 to AP-1 activation is the direct phosphorylation and activation of other factors.[27] Activated AP-1 has been thought to play a dominant role in the transcriptional activation of MMP promoters.[28] Similar to previous studies, we saw that phosphorylation of JNK, ERK, and p38 kinases was activated with UVB irradiation, followed by translocation to the nucleus and activation of c-Jun and c-Fos phosphorylation. Our data indicated that PVE significantly inhibited the expression of

p-JNK and p-ERK and alleviated the phosphorylation of c-Jun and c-Fos in a dose-dependent manner.

Meanwhile, ROS stimulates multiple growth factor receptors and cell surface cytokines, activating transcription factor NF-κB subunits into the nucleus and transcriptionally upregulating various proinflammatory target proteins, such as IL-6 and TNF-α.[29] In addition, MAPKs also regulate inflammatory gene transcription,[30] and NF-κB is also involved in the transcriptional regulation of UVB-induced MMP-1 and MMP-3 expression.[31] This crosstalk between NF-κB and MAPKs under oxidative stress has garnered recent interest. We observed that UVB induced the excessive production of ROS, leading to secretion of IL-6 and TNF-α and prompting NF-κB activation. Treatment with PVE effectively alleviated UVB-induced ROS upregulation of IL-6 and TNF-α mRNA levels and then reduced the expression of NF-κB resulting in overall anti-inflammatory activity. In addition, our MTT results showed that PVE was not cytotoxic to NHDFs, making PVE a good potential natural anti-inflammatory drug for the skin.

Taken together, our findings indicated that PVE suppressed MMPs expression through inhibition of the AP-1 signaling pathway, which is regulated by the JNK and ERK proteins in NHDFs. PVE also displayed anti-inflammatory activity by suppressing ROS release to relieve the levels of IL-6 and TNF-α, effectively inhibiting NF-κB expression. PVE counteracted photoaging, mainly by promoting the TGF-β1/Smad-dependent transcriptional activation of procollagen type I, and advanced TGF/Smad pathway signaling by improving the protein level of Smad 2/3 and reducing Smad 7 expression. These data indicate PVE might have applications as a complementary and alternative medicine for prevention of skin photo-oxidation.

Conclusion

In the present study, PVE protected NHDFs from UVB-induced inflammatory and photoaging damage by inhibiting MAPKs, AP-1, and NF-κB signaling and promoting the TGF-β1/Smad pathway.

Acknowledgment

This work was supported by the TAEYI Life Science Co. Ltd., Republic of Korea.

Author Disclosure Statement

No competing financial interests exist.

References

1. Amaro-Ortiz A, Yan B, D'Orazio JA. Ultraviolet radiation, aging and the skin: Prevention of damage by topical cAMP manipulation. Molecules 2014;19:6202–6219.
2. Zhang W, Liu HT. MAPK signal pathways in the regulation of cell proliferation in mammalian cells. Cell Res 2002;12:9.
3. Lu Z, Xu S. ERK1/2 MAP kinases in cell survival and apoptosis. IUBMB Life 2006;58:621–631.
4. Rodríguez-Berriguete G, Fraile B, Martínez-Onsurbe P, Olmedilla G, Paniagua R, Royuela M. MAP kinases and prostate cancer. J Signal Transduct 2011;2012:169170.
5. Cargnello M, Roux PP. Activation and function of the MAPKs and their substrates, the MAPK-activated protein kinases. Microbiol Mol Biol Rev 2011;75:50–83.
6. Son Y, Kim S, Chung HT, Pae HO. Reactive oxygen species in the activation of MAP kinases. Methods Enzymol 2013;528: 27–48.
7. Pittayapruek P, Meephansan J, Prapapan O, Komine M, Ohtsuki M. Role of matrix metalloproteinases in photoaging and photocarcinogenesis. Int J Mol Sci 2016;17:868.
8. Fisher GJ, Shao Y, He T, Qin Z, Perry D, Voorhees JJ, Quan T. Reduction of fibroblast size/mechanical force down-regulates TGF-β type II receptor: Implications for human skin aging. Aging Cell 2016;15:67–76.
9. Klingberg F, Chow ML, Koehler A, Boo S, Buscemi L, Quinn TM, Costell M, Alman BA, Genot E, Hinz B. Prestress in the extracellular matrix sensitizes latent TGF-β1 for activation. J Cell Biol 2014;207:283–297.
10. Quan T, Shao Y, He T, Voorhees JJ, Fisher GJ. Reduced expression of connective tissue growth factor (CTGF/CCN2) mediates collagen loss in chronologically aged human skin. J Invest Dermatol 2010;130:415–424.
11. Luckett-Chastain LR, Cottrell ML, Kawar BM, Ihnat MA, Gallucci RM. Interleukin (IL)-6 modulates transforming growth factor-β receptor I and II (TGF-βRI and II) function in epidermal keratinocytes. Exp Dermatol 2016; DOI: 10.1111/exd.13260.
12. Lee YR, Noh EM, Jeong EY, Yun SK, Jeong YJ, Kim JH, Kwon KB, Kim BS, Lee SH, Park CS, Kim JS. Cordycepin inhibits UVB-induced matrix metalloproteinase expression by suppressing the NF-κB pathway in human dermal fibroblasts. Exp Mol Med 2009;41:548.
13. Martinez RM, Pinho-Ribeiro FA, Steffen VS, Caviglione CV, Vignoli JA, Barbosa DS, Baracat MM, Georgetti SR, Verri Jr WA, Casagrande R. Naringenin inhibits UVB irradiation-induced inflammation and oxidative stress in the skin of hairless mice. J Nat Prod 2015;78:1647–1655.
14. Hwang E, Park SY, Lee HJ, Lee TY, Sun ZW, Yi TH. Gallic acid regulates skin photoaging in UVB-exposed fibroblast and hairless mice. Phytother Res 2014;28:1778–1788.
15. Sun Z, Park SY, Hwang E, Zhang M, Seo SA, Lin P, Yi TH. *Thymus vulgaris* alleviates UVB irradiation induced skin damage via inhibition of MAPK/AP-1 and activation of Nrf2-ARE antioxidant system. J Cell Mol Med 2017;21: 336–348.
16. Hwang E, Ngo HT, Park B, Seo SA, Yang JE, Yi TH. Myrcene, an aromatic volatile compound, ameliorates human skin extrinsic aging via regulation of MMPs production. Am J Chin Med 2017;45:1113–1124.
17. Huang R, Zhao M, Yang X, Huang J, Yang Y, Chen B, Tan J, Huang J, Li Z, Lv Y, Ji G. Effects of *Prunella vulgaris* on the mice immune function. PLoS One 2013;8:e77355.
18. Masaki H. Role of antioxidants in the skin: Anti-aging effects. J Dermatol Sci 2010;58:85–90.
19. Feng L, Jia X, Zhu MM, Chen Y, Shi F. Antioxidant activities of total phenols of *P. vulgaris* L. in vitro and in tumor-bearing mice. Molecules 2010;15:9145–9156.
20. Chen Y, Zhu Z, Guo Q, Zhang L, Zhang X. Variation in concentrations of major bioactive compounds in *P. vulgaris* L. related to plant parts and phenological stages. Biol Res 2012;45:171–175.
21. Lamaison J, Petitjean-Freytet C, Carnat A. Medicinal Lamiaceae with antioxidant properties, a potential source of rosmarinic acid. Pharm Acta Helv 1991;66:185.
22. Zdarilová A, Svobodová A, Simánek V, Ulrichová J. *P. vulgaris* extract and rosmarinic acid suppress lipopolysaccharide-induced alteration in human gingival fibroblasts. Toxicol In Vitro 2009;23:386–392.

23. da Cunha FM, Duma D, Assreuy J, Buzzi FC, Niero R, Campos MM, Calixto JB. Caffeic acid derivatives: In vitro and in vivo anti-inflammatory properties. Free Radic Res 2004;38:1241–1253.
24. Saija A, Tomaino A, Lo Cascio R, Trombetta D, Proteggente A, De Pasquale A, Uccella N, Bonina F. Ferulic and caffeic acids as potential protective agents against photooxidative skin damage. J Sci Food Agric 1999;79:476–480.
25. Meng XM, Nikolic-Paterson DJ, Lan HY. TGF-[beta]: The master regulator of fibrosis. Nat Rev Nephrol 2016;12:325–338.
26. Yan X, Chen YG. Smad7: Not only a regulator, but also a cross-talk mediator of TGF-β signaling. Biochem J 2011; 434:1–10.
27. Tanos T, Marinissen MJ, Leskow FC, Hochbaum D, Martinetto H, Gutkind JS, Coso OA. Phosphorylation of c-Fos by members of the p38 MAPK family role in the AP-1 response to UV light. J Biol Chem 2005;280:18842–18852.
28. Vincenti MP, Brinckerhoff CE. Transcriptional regulation of collagenase (MMP-1, MMP-13) genes in arthritis: Integration of complex signaling pathways for the recruitment of gene-specific transcription factors. Arthritis Res 2001;4:157.
29. Mishra V, Baranwal V, Mishra RK, Sharma S, Paul B, Pandey AC. Titanium dioxide nanoparticles augment allergic airway inflammation and Socs3 expression via NF-kB pathway in murine model of asthma. Biomaterials 2016;92: 90–102.
30. Arthur JSC, Ley SC. Mitogen-activated protein kinases in innate immunity. Nat Rev Immunol 2013;13:679–692.
31. Bond M, Baker AH, Newby AC. Nuclear factor κB activity is essential for matrix metalloproteinase-1 and-3 upregulation in rabbit dermal fibroblasts. Biochem Biophys Res Commun 1999;264:561–567.

Address correspondence to:
Tae-Hoo Yi
SD Biotechnologies Co., Ltd.
#301 Seoul Hightech Venture Center
29, Gonghang-daero 61-gil
Ganseo-gu
Seoul 07563
Korea

E-mail: drhoo@khu.ac.kr

Received: April 14, 2017
Accepted: January 29, 2018